

Małgorzata Węclawek¹, Dariusz Ziora², Dariusz Jastrzębski²¹Pulmonology Department, Public Clinical Hospital No. 1 in Zabrze, Silesia Medical University in Katowice, Zabrze, Poland²Department of Lung Diseases and Tuberculosis, School of Medicine with the Division of Dentistry in Zabrze, Medical University of Silesia in Katowice, Poland

Imaging methods for pulmonary sarcoidosis

Abstract

Sarcoidosis is a chronic systemic granulomatous disease of unknown etiology. In more than 90% of patients with diagnosed sarcoidosis, mediastinal and hilar lymph nodes are affected. The objective of this paper is to discuss the most important chest imaging methods in pulmonary sarcoidosis. A chest X-ray remains the method of choice at both the diagnostic stage and during follow-up of the disease progress. High-resolution computed tomography allows for a more thorough description of lesions in terms of their location. Research demonstrates the superiority of FDG PET over both aforementioned techniques in the assessment of active inflammatory lesions. Magnetic resonance imaging is currently being used in diagnosing cardiac sarcoidosis. Although EBUS constitutes the basic diagnostic tool, the invasiveness of the method results in it not being used when monitoring the activity of the disease.

Key words: X-ray, HRCT, PET/CT, MRI, scintigraphy, pulmonologist point of view

Adv Respir Med. 2020; 88: 18–27

Introduction

Sarcoidosis is a chronic granulomatous disease of unknown etiology [1]. In more than 90% of patients with diagnosed sarcoidosis, mediastinal and hilar lymph nodes are affected [2, 3]. The diagnosis is based on the evaluation of clinical, radiological, and histopathological features [7]. The objective of this paper is to discuss the most important chest imaging methods in pulmonary sarcoidosis and to determine their role in the process of diagnosing the disease and monitoring its activity.

Conventional X-ray

The method of choice which should be applied in each and every patient with a clinical suspicion of sarcoidosis is a conventional X-ray [8]. Its unquestionable advantages include its wide availability and low cost. Despite the development of other techniques, X-ray imaging remains the first examination recommended in the diagnostic procedure, and a gold standard in

monitoring the activity of the already diagnosed disease [8]. It is recommended to apply relevant scales in order to systematise and standardise X-ray images. One of the best-known scales is the one proposed by Scadding/Siltzbach in 1961 in which patients were classified according to one of four groups based on lesions visible in the chest X-ray (i.e. enlarged hilar lymph nodes, the presence of parenchymal infiltrations, and features of fibrosis) [9]. The first group included patients with isolated hilar lymphadenopathy; the second — subjects with accompanying parenchymal infiltrations; the third — subjects without lymphadenopathy, but with lesions in the lung parenchyma; the fourth — patients with fibrotic lesions. On the basis of the group of patients ($n = 136$), Scadding rated the incidence of individual groups in the population of patients with sarcoidosis and the probability of spontaneous remission in each of them [9]. This scale was accepted and has been widely used to date. Another classification method, which was applied in the analysis of pneumoconiosis and adapted by Muers *et al.*, consists of the division of both lung

Address for correspondence: Małgorzata Węclawek, Pulmonology Department, Public Clinical Hospital No. 1 in Zabrze, Silesia Medical University in Katowice, Zabrze, Poland;

e-mail: mweclawek@szpital.zabrze.pl

DOI: 10.5603/ARM.2020.0074

Received: 02.10.2019

Copyright © 2020 PTChP

ISSN 2451–4934

lobes into zones and in the evaluation of the profusion of individual types of lesions in the zones, specifically reticulonodular changes, masses, confluents, and fibrosis [10, 11]. The chest X-ray and the pulmonary function test (PFT) constitute the main tools for monitoring the activity of sarcoidosis. Boros *et al.* retrospectively analyzed the results of functional tests in 830 patients with diagnosed sarcoidosis. They analyzed them based on the stage that they were in determined by the Scadding/Siltzbach classification of chest X-ray [12]. Despite the parenchymal changes visible in the chest X-ray in about three-quarters of patients (stages II–IV), only 7% had a restriction in lung volume. At each stage (according to Scadding/Siltzbach), the lung transfer factor for carbon monoxide was impaired and static lung compliance was reduced [12]. Despite an established position which identifies X-ray imaging as a tool for monitoring the disease, the discussion devoted to decision making with reference to the onset of therapy based exclusively on the basis of radiological changes without accompanying lung function disorders is still ongoing. Pietinalho *et al.*, in their study of patients with recently diagnosed sarcoidosis that had no deviations in the functional tests, applied a 3 months' therapy with prednisone, which was followed by inhaled budesonide for 15 months. They demonstrated that patients, who at the onset of the therapy had stage II/III sarcoidosis and received treatment, experienced specific benefits in terms of FVC and DLCO 5 years after the study. Furthermore, they required glucocorticosteroid therapy much later than when compared to the placebo group [5]. Considering the possible side effects of the therapy, it is recommended to exercise caution when deciding about the beginning and/or continuation of treatment based exclusively on the advancement of the disease as evaluated in the chest X-ray. Figure 1 presents typical conventional chest X-ray picture of stage II sarcoidosis.

High resolution computed tomography

A method that has become much more accessible is computed tomography. High-resolution computed tomography (HRCT), which is a method of choice in the evaluation of interstitial diseases, demonstrates a considerable superiority over the CT with contrast in the detection and evaluation of even subtle lesions in lung parenchyma [14]. Routine diagnostic protocols make use of thin-layer scans, from 1 to 1.5–2 mm [15]. In the past, the “so-called” sequential HRCT scans

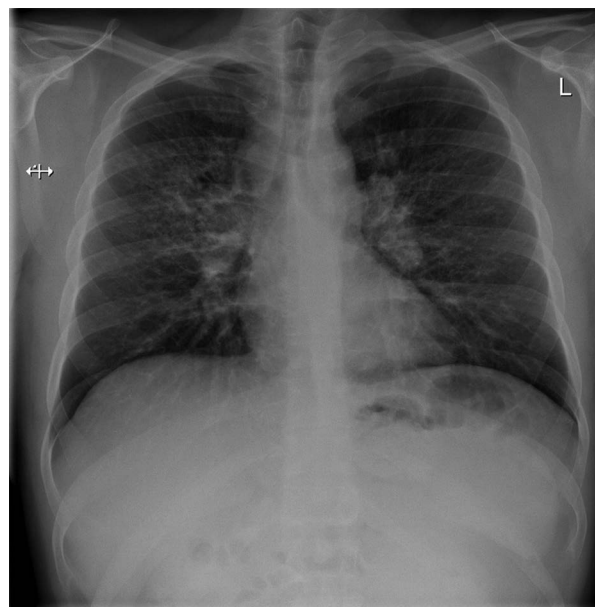


Figure 1. Chest X-ray of the patient with stage II sarcoidosis. Enlarged bilateral hilar lymph nodes, widening of mediastinum and bilateral nodular shadows spreading from perihilar regions to the lung periphery

were used where layers were visualized every 10 mm from the apex of the lung to its base at full inspiration. As a result, as much as 90% of the lung was not seen on imaging. Thanks to advanced technical devices (multiple detector computed tomography), the rotation time necessary to generate the image has been shortened to 0.28–0.5 seconds (depending on the type of the apparatus). The use of spiral acquisition enhanced the scan sensitivity and minimised respiratory and pulsatory artefacts [15, 16, 17]. According to the 1999 ATS/ERS/WASOG guidelines which are still valid, there are three indications to perform a CT scan: a) if there are no lesions in the X-ray, but there is a clinical suspicion of sarcoidosis (stage 0); b) if there are atypical clinical or radiological symptoms; and c) in order to diagnose possible complications [1]. There are two typical findings in sarcoidosis in HRCT. Firstly, there is hilar and mediastinal lymphadenopathy which is most frequently bilateral and symmetrical. Secondly, there are nodules (both micronodules [2–4 mm in diameter] and macronodules (diameter \geq 5 mm)) which can be located along bronchovascular bundles, interlobular septi, interlobar fissures, and in the subpleural region (Figure 2) [18]. In advanced stages, the features of fibrosis are visible and can include honeycombing, architectural distortion, traction bronchiectasis, and/or volume loss. Most frequently, lesions in sarcoidosis demonstrate predilection to the upper and middle fields [18].

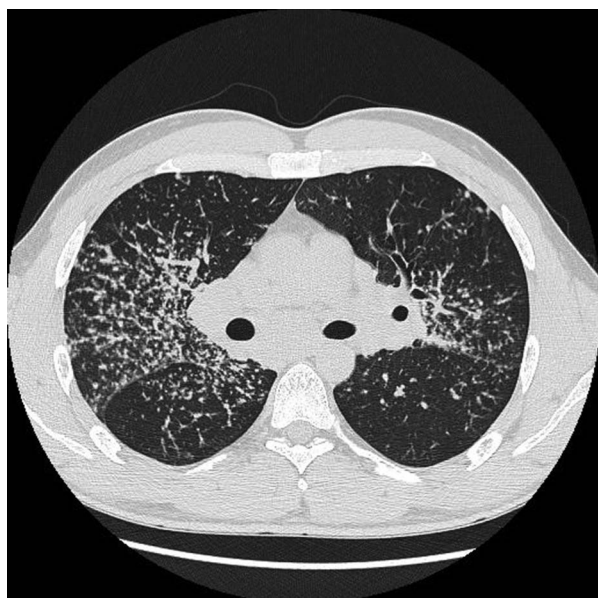


Figure 2. Chest high resolution computed tomography of the patient with stage II sarcoidosis. Enlarged hilar and subcarinal lymph nodes, disseminated high density nodules in both middle lung areas, with peribronchovascular and subpleural distribution

The increasingly widespread application of the HRCT scan is associated with better-known radiological characteristics of sarcoidosis. Cases of histopathologically confirmed sarcoidosis with atypical manifestations in the HRCT scan are becoming more and more frequent. Sarcoidosis has been dubbed “the great imitator”, just like tuberculosis before it [19, 20]. More and more authors present cases of patients with new CT patterns [21]. Radiological manifestations less frequently encountered in sarcoidosis but seen on HRCT include unilateral or isolated lymphadenopathy, parenchymal infiltrations in the form of conglomerate masses, single nodules larger than 1 cm, confluent alveolar opacities (alveolar sarcoid pattern), and cavernous changes [18]. An interesting symptom is that of granulomatous nodules coalescing together to form larger ones, which was described for the first time by Nakatsu *et al.* [21]. Bigger nodules are surrounded by smaller satellite nodules forming a structure resembling stars forming a galaxy, hence the galaxy symptom mentioned by the authors. In the study, this symptom was found in 16 out of 59 subjects. The 3-mm collimation was used for the evaluation of the larger nodules (instead of conventionally used 1–2 mm layer) which, in the authors’ opinion, had a positive effect on the visualisation of peripheral micronodules, bronchioles, and branches thereof [21]. Another relatively new image of sarcoidosis in HRCT is the “sarcoid cluster sign”

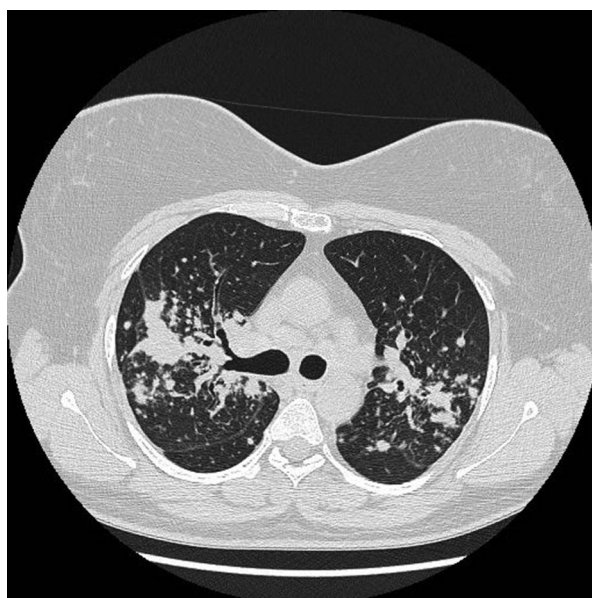


Figure 3. Chest high resolution computed tomography showing coalescent nodules forming larger irregular nodes — “galaxy sign”

which was first described by Herráez Ortega. This sign is characterised by the accumulation of small punctiform nodules on the periphery of the lungs [22]. However, both “galaxy” and “cluster” signs can be seen in pulmonary TB and silicosis as well (Figure 3) [23–25].

According to the authors, the majority of such lesions are arranged in circular groups and are not located directly in subpleural peripheral regions of the upper and middle fields of the lungs [22]. Other patterns visible in HRCT have been also described such as “reversed halo” ring-shaped areas of consolidation with a central ground-glass attenuation [26–29]. Besides the precise assessment of the profusion of interstitial lesions, HRCT also indirectly allows to assess the prognosis for patients suffering from sarcoidosis by differentiating between reversible and irreversible lesions [30]. Lesions such as micronodules, nodules, or peribronchovascular thickening can withdraw spontaneously or under treatment. On the other hand, consolidations, ground-glass opacification, or linear opacities are characterised by variable reversibility. Irreversible lesions include architectural distortion, bronchiectasis, honeycombing, and emphysematous bullae (Figure 4) [31]. The role of HRCT in diagnosing sarcoidosis, particularly in cases which are difficult to diagnose, is currently broadly recognised. There is an ongoing discussion regarding the role of computed tomography in the monitoring of the activity of

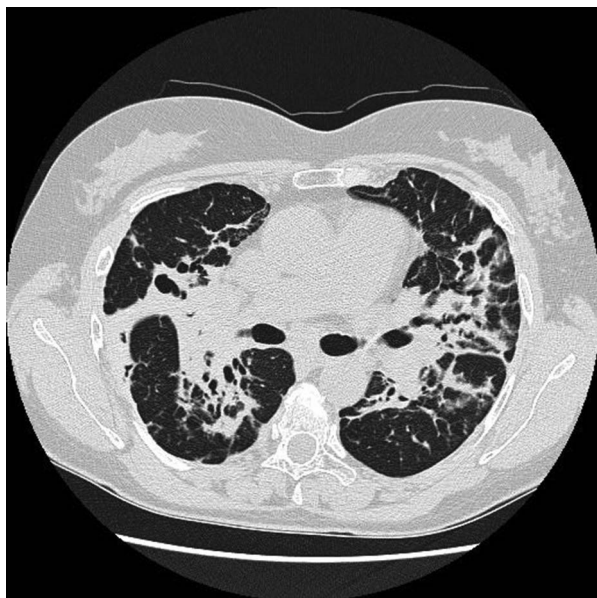


Figure 4. Lung fibrosis in sarcoidosis. Severe architectural distortion

the disease. This discussion is attempting to determine whether it should be repeated routinely in every patient, whether it should be applied only in the case of more advanced lesions visible on an X-ray, and whether it should be used in the presence of functional disorders. Ziora *et al.* analysed a group of patients who would have fallen into group 1 according to the Scadding scale. After examining these patients by HRCT, they assigned them to two separate subgroups: patients with lesions in pulmonary parenchyma, and patients without parenchymal lesions [32]. Both groups underwent regular functional testing and X-ray scans. During a 2-year long observation, no statistically significant difference was observed between the functional test results. Moreover, the share of patients with radiological stabilisation, progression, or improvement was not different in both groups [32]. Numerous studies have demonstrated the superiority of HRCT in detecting lesions corresponding to fibrosis and in diagnosing more advanced stages of the disease. Chest X-ray scans revealed fibrosis in 5–10%, whereas CT scans resulted in such changes being described in as many as 20–50% of patients [33–35]. Currently, there are no clear data which would allow to determine whether repeated HRCT scans in patients suffering from sarcoidosis have any effect on making therapeutic decisions. Levy *et al.* recommend repeated HRCT scans if the clinical image changes or complications are suspected [36–37]. Unlike X-ray scans, some lesions visible in HRCT demonstrate a relationship with pulmonary

function disorders [38–40]. Drent *et al.* demonstrated correlations between features visible in HRCT such as thickening of the bronchovascular bundle, intraparenchymal nodules, septal and non-septal lines, or focal pleural thickening on one hand, and results of respiratory functional tests on the other [38]. However, such a relationship has not been demonstrated for consolidations, ground-glass opacifications, or enlargement of lymph nodes. Furthermore, the study also demonstrated the superiority of the HRCT scan over a conventional X-ray scan in terms of their relationship to the respiratory function parameters of the lungs [38].

Gallium-67 scintigraphy

Another imaging method used in sarcoidosis is Gallium-67 scintigraphy (Ga-67), albeit less and less frequently so. Its sensitivity in detecting pulmonary sarcoidosis ranges from 60 to 90% [41, 42]. For patients suffering from sarcoidosis, two gallium uptake patterns are characteristically used known as lambda and panda, and are named as such because of their shapes [43]. The lambda pattern comprises the gallium uptake in the parahilar and infrahilar lymph nodes along with the paratracheal lymph nodes on the right-hand side [43]. The panda pattern is associated with a symmetrical uptake in parotid and lacrimal glands, as well as in submandibular and sublingual salivary glands. The constellation of the lambda and panda pattern uptake is recognised as very characteristic for sarcoidosis [17, 44]. Gallium-67 scintigraphy is more sensitive than an X-ray scan and can be applied for the evaluation of the staging of the disease activity, for the assessment of treatment results, and for the prediction of relapses. However, a more widespread application of this method is limited due to its restricted availability, cost, exposure to radiation, and duration [43].

Scintigraphy with other tracers

It is also possible to use scintigraphy with other tracers. Somatostatin receptor (SR) scintigraphy is based on the uptake of octreotide derivatives, such as ^{99m}Tc -octreotide or other somatostatin derivatives, by somatostatin subtype 2 receptors. The application of this method affected therapeutic decisions of Piotrowski *et al.*, who in their study compared the predictive value of scintigraphy with ^{99m}Tc -octreotide and biomarkers (SACE, CRP, markers of calcium metabolism, lymphocytes in BALF, 8-isoprostane in exhaled

breath condensate) [45]. The authors observed the uptake in the area of pulmonary parenchyma in patients who had been previously disqualified from treatment. The attempted therapy in such patients was associated with a partial regression of interstitial changes. However, it was decided to terminate the treatment in patients subjected to long-term therapy with glucocorticosteroids who also had a negative scintigraphy result. In relation to the biomarkers, a significantly higher level of EBC 8-IP was demonstrated in patients with a positive uptake in scintigraphy as compared to patients with a negative scintigraphy result. Furthermore, a positive correlation between the uptake ratio and the level of SACE in the group of patients with a positive scintigraphy result was observed [45]. French authors compared gallium scintigraphy with SRS in a group of 18 patients with recognized sarcoidosis. SRS appears to be accurate and contributes to a better evaluation of organ involvement in sarcoidosis patients, especially those treated with corticosteroids [46].

Single-photon emission computed tomography

The image of classical scintigraphy is obtained by projecting a three-dimensional object onto a plane. This technique is extended by the use of several gamma cameras rotating around the patient, which allows to obtain an image of selected layers. This method, referred to as single-photon emission computed tomography (SPECT), was applied by Vis *et al.* [47]. The SPECT/CT scan was performed in a group of 10 patients after the administration of technetium-99m(99mTc)-labelled infliximab. The patients demonstrated a correlation between the radiomarker accumulation in SPECT and the lab parameters (sIL-2R, ACE level in serum, ACE Z-score, CD4/CD8 level in BAL), functional test disorders, as well as the PET scan with fluorodeoxyglucose. The study demonstrated variable selective accumulation of the radiomarker in SPECT, which correlated positively with the lab markers and negatively with the pulmonary function, as well as with the PET scan [47]. A similar result was also obtained by — without limitations — Galli *et al.*, who demonstrated a negative correlation between the uptake of 99mTc-labelled infliximab and the activity measured in the PET scan. The scan with the application of ^{99m}Tc-labelled infliximab with the TNF alpha inhibitor may be used in the future to select groups of patients where this therapy will be effective. However, further research into this subject is required [48].

Positron-emission tomography

Another study in the field of nuclear medicine is positron-emission tomography (PET). Simultaneous use of computed tomography allows to shorten the duration of the scan and additionally improve the accuracy of descriptions of anatomical changes detected (PET/CT) [49]. The most commonly used marker is ¹⁸F-FDG, which is a glucose analogue. Transported through the cell membrane inside the cell, it is subjected to phosphorylation by hexokinase. Consequently, a molecule of 18F-FDG-6 phosphate is formed and it is not metabolised any further. The accumulation of macrophages exhibiting increased metabolism in the area of sarcoid granulomas causes an uptake of the administered marker by glucose transporters GLUT-1 and GLUT 3 [50]. The superiority of 18F-FDG PET/CT over Gallium-67 scintigraphy was demonstrated by Braun *et al.* in their study. They confirmed the very high sensitivity of the former in detecting active foci within the chest reaching 100%, as compared to 71% when scintigraphy is applied [49]. In addition, the advantages of FDG-PET include having 3 times lower radiation dose and shorter time of procedure [51].

The research points to a good correlation between an X-ray and PET scan in the case of higher stages of sarcoidosis according to the Scadding scale [52]. A chest X-ray showing no lesion, which stands for stage 0 in this classification, does not exclude a positive result of the PET scan. In the study of Mostard *et al.*, in 27% of patients with no symptoms in the chest X-ray, a marker uptake was detected. In advanced stage 4 patients, activity was also visible in the PET scan for the majority of subjects (88%) [51]. The study also compared HRCT (on the basis of the score proposed by Oberstein) with images obtained in PET scans (occurrence/non-occurrence of changes). In this case, patients with the score 0, according to Oberstein, did not have any changes visible in the PET scan. Conversely, in subjects where HRCT scan revealed features of fibrosis, the activity was frequently visible in the PET scan. This may be indicative of a still active and potentially reversible inflammatory process [52]. The selection of patients in which the inflammatory process is still ongoing despite fibrosis having been found may allow clinicians to choose the optimum treatment in this group of patients. PET can be applied in the diagnostic procedure of the disease; it allows to detect active inflammatory lesions in patients with symptoms,

even if other diagnostic methods give negative results. PET also identifies the best locations for biopsy. It is used for monitoring the activity of the disease, and diffuse parenchymal infiltrations detected in this scan allow to predict further loss of the pulmonary activity [53, 54]. Sobic-Saranovic *et al.* demonstrated that in a group of 90 patients subjected to ^{18}F -FDG PET/CT scans, 81% of them had decisions regarding further treatment made based on the scan result. In the majority of patients in which an increased marker uptake was observed in the PET scan, the previously administered dosage of glucocorticosteroids was increased or a new medication was used. On the other hand, patients with a negative scan result had their dosage reduced or the medications were discontinued altogether [55]. PET can be helpful in deciding whether patients with severe sarcoidosis should receive biological treatment. In the study by Vorselaars *et al.*, a PET scan was performed prior to the onset of therapy and then again after 26 weeks [56]. The second follow-up scan revealed a reduction of the standardised uptake value in the region of mediastinum by 2.97 ($P < 0.0001$), and in the region of lung parenchyma by 3.93 ($p < 0.0001$) as compared to the output SUV values. The higher the SUV values were prior to the administration of infliximab, the greater the improvement was in terms of the FVC values observed after treatment [56].

The role that PET can play in the evaluation of the activity of the disease in the future is pointed to by the study comparing the serological markers of the activity of the disease used so far, such as ACE and soluble interleukin 2 receptor [57]. In a retrospective study, 36 patients with recently diagnosed symptomatic disease had a PET scan performed and their levels of ACE and sIL-2R were measured. F-FDG PET was positive in as many as 34 out of 36 patients (94%), elevated levels of ACE were observed in 13 patients (36%), and increased sIL-2R in 17 (47%) [57].

Additional benefits offered by a PET scan also include the extent of the examination which covers the entire body and can sometimes allow to find sarcoid foci in other organs. This scan can constitute an alternative for patients with suspected cardiac sarcoidosis in whom an MRI scan cannot be performed (e.g. due to the presence of a pacemaker or ICD) [53].

Unfortunately, the uptake of ^{18}F -FDG occurs in sarcoid as well as neoplastic lesions. Therefore, this examination is not suitable for differentiating between sarcoidosis and neo-

plasms. A group of Japanese researchers raised the subject of using another marker, ^{18}F -FMT (Fluorine-18- α -Methyltyrosine) [58]. The study covered a group of 24 patients with sarcoidosis that also had an additional suspicion of a neoplastic process occurring. The control group included patients with diagnosed lung cancer. In all the subjects from the examined group, the uptake of ^{18}F -FDG in lymph nodes was observed, whereas ^{18}F -FMT was not accumulated in them. In extranodal organs, such as the liver, spleen, and bones, the PET scan result was positive if the former marker was used and negative with the latter. The neoplastic disease was not diagnosed in any of the study subjects [58]. The mean standardised uptake values (SUV) in the examined group for ^{18}F -FDG and ^{18}F -FMT were 5.01 ± 2.15 and 0.77 ± 0.24 respectively, whereas in the control group consisting of patients suffering from the neoplastic disease the values were 6.34 ± 2.52 for ^{18}F -FDG and 1.54 ± 0.82 for ^{18}F -FMT. On the basis of these results, the authors concluded that the additional use of ^{18}F -FMT besides ^{18}F -FDG may facilitate the differentiation between sarcoid and malignant changes [58]. Like is the case with Gallium-67 scintigraphy, the common use of PET and PET/CT scans is limited due to their limited availability and high costs. Figures 5 and 6 present PET results of patients with sarcoidosis.

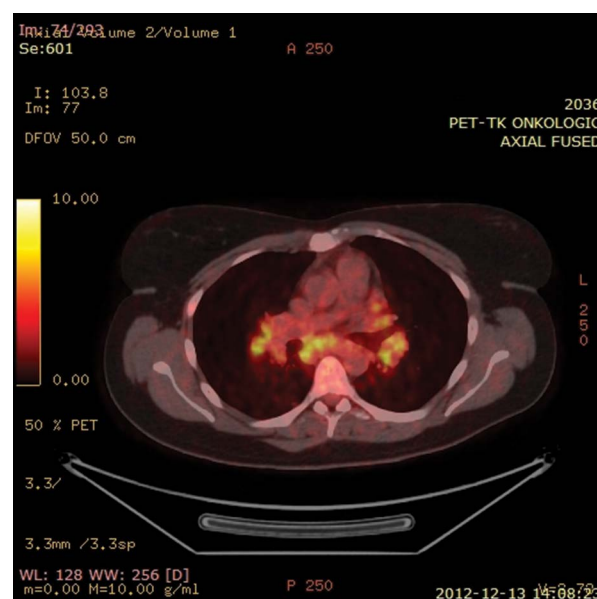


Figure 5. PET-CT axial view showing increased ^{18}F -FDG uptake in both hilar and subcarinal lymph nodes. The patient was suspected of lymphoma, after endobronchial ultrasound (EBUS) transbronchial needle biopsy sarcoidosis was confirmed

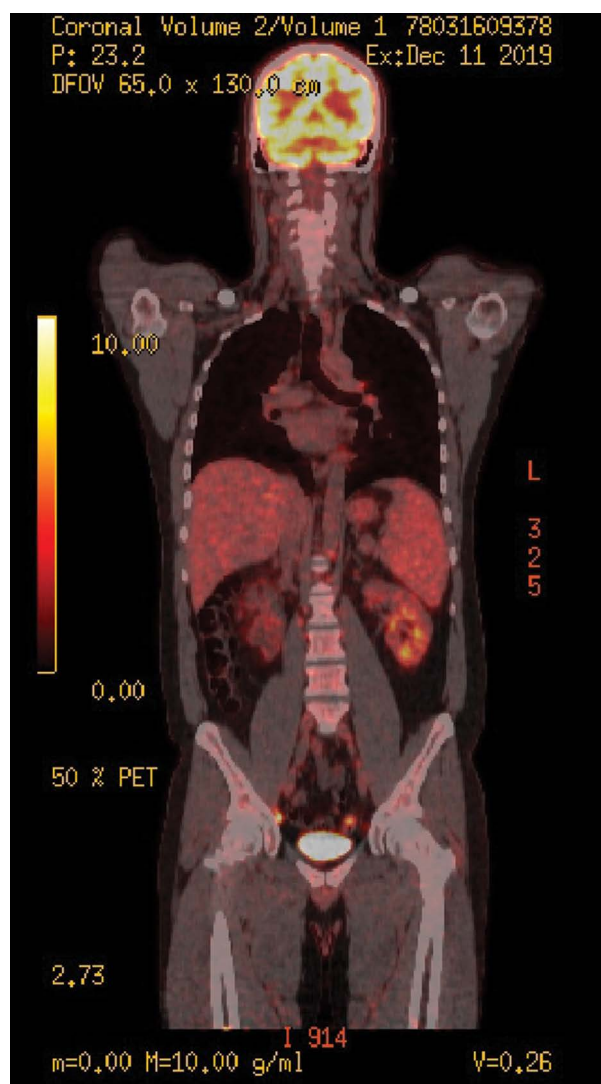


Figure 6. PET-CT coronal view. The patient with chronic sarcoidosis, presenting signs of radiological remission in most recent CT. PET was performed to exclude suspected extrathoracic manifestation of sarcoidosis. Increased uptake of 18F-FDG in cervical, intrathoracic and pelvic lymph nodes

Magnetic resonance imaging

Magnetic resonance imaging (MRI) is a recognised imaging method in the diagnostic procedure of cardiac sarcoidosis and in evaluating changes in the structure of bones or in the central nervous system, but it is rarely applied for the evaluation of the lung parenchyma due to the limitations of this method associated with the presence of air in the lung tissue and the physiological motion of the chest (cardiac pulsation, respiration) [17, 59–61]. Most studies have demonstrated the superiority of HRCT over MRI in the evaluation of interstitial lesions

[17]. Brady *et al.*, who used the technique of late enhancement in magnetic resonance imaging in their work, obtained comparable results when using HRCT and MRI in the description of lesions suggestive of fibrosis [62]. Consistency between MRI and HRCT in the diagnosis of pulmonary sarcoidosis was also confirmed by Chung *et al.*, who evaluated images in terms of the presence of interstitial changes, reticulations, nodules, and condensations according to a 3-point scale in the division into lobes. Furthermore, they noticed that a better correlation between the scans related to the upper lobes [63]. In relation to lymphadenopathy, MRI is a technique demonstrating a similar value to computed tomography in detecting enlargement of hilar and mediastinal lymph nodes. Nevertheless, MRI facilitates the evaluation of the extent of lymphadenopathy as it is differentiated better from the vascular system of the lungs [64]. Chung *et al.*, referred to above, analysed MRI scans performed in the heart examination protocol and noticed that some patients with sarcoidosis had lymph nodes with a specific appearance: a hypo-intensive signal inside and a hyper-intensive rim. This symptom was called a dark lymph node sign by the authors. Retrospectively, it occurred in 49% of patients from the examined group [65]. New signs being described in MRI scans give hope for better characteristics of sarcoidosis based on MRI and potentially, for a more common use of this method in the future.

Endoscopic ultrasonography

Many studies assessing the possibility of using endoscopic ultrasonography in the evaluation of lymph nodes in patients suffering from sarcoidosis have been conducted in recent years. EBUS/EUS already enjoys an established position in the diagnosis of sarcoidosis [4–6]. EBUS allows to evaluate 2R, 4R lymph nodes on the right-hand side, 2L, 4L lymph nodes on the left-hand side, as well as paratracheal and subcarinal regions (group 7). Additionally, EBUS helps to access hilar lymph nodes (group 10) and the interlobar region of group 11. An EUS scan allows to examine the subcarinal region 7, the paraesophageal region 8, and region 9. It is also possible to access the paratracheal region on the left-hand side (4L), and to partially assess the left hilar region as well (10 L). A meta-analysis covering 14 studies (which covered 2097 subjects in total) demonstrated a high diagnostic efficiency of this method,

reaching 79%. Its sensitivity and specificity were estimated to be 84% and 100%, respectively [66]. The percentage of positive results obtained thanks to the EBUS-TBNA method is higher in patients with stage 1 than 2, which probably results from a higher density of granulomas in stage 1. EBUS allows not only to collect the material, but also to evaluate lymph nodes. In their study, Erol *et al.* compared the image of lymphadenopathy in tuberculosis and sarcoidosis [67]. Lymph nodes in sarcoidosis formed conglomerates more often than in tuberculosis and were also characterised by higher homoechogenicity. In tuberculosis, lymph nodes were more frequently oval in shape and more heterogenous, and their foci of necrosis were bigger as well. Due to the fact that both diseases belong to the group of granulomatous diseases, lymph nodes had a similar vascular pattern [67]. Agrawal *et al.* compared inter alia metastatic lymph nodes with lymph nodes enlarged due to sarcoidosis. In this case, features that differentiated lymph nodes in the course of proliferative diseases from sarcoid ones were predominantly heterogenicity, clear margins, signs of coagulative necrosis, and the presence of the central hilar structure (CHS) [68]. Regrettably, due to the invasiveness of this method, it cannot be practically used in the monitoring of the activity of the disease [69].

Transthoracic ultrasound scan

Nowadays, advanced high-resolution ultrasound apparatuses with facultative employment of colour Doppler allow to examine the mediastinum and the heart region. In their study, Hirche *et al.* compared the application of a transthoracic ultrasound scan with a conventional X-ray scan [70]. The use of an ultrasound scan in the evaluation of mediastinal lymph nodes proved to be up to 90% effective. Lymph nodes in patients who on the basis of a chest X-ray had been assigned to groups 1–3 according to the Scadding score were particularly well visible. This is in contrast to group 4, in which the ultrasound visualisation of lymph nodes turned out to be insufficient. A benefit stemming from this method is the fact it allows for a morphological assessment of the lymph nodes, which is not possible based on an X-ray scan. In the study summary, however, the authors emphasise that the sensitivity of this method in detecting lymphadenopathy is highly dependent on the experience and skills of the operator and the class of the device [70].

Conclusion

Currently, we have observed constant progress in the field of imaging. Thanks to the development of advanced techniques, it is possible to understand sarcoidosis better, to grasp its natural course and the effect of treatment onto the activity of the changes. A chest X-ray scan remains the basic examination at the stage of diagnosis, as well as in the subsequent monitoring of the disease. High-resolution computed tomography allows for a more precise description of lesions with reference to their location. Studies point to the superiority of FDG PET over both methods in the evaluation of active inflammatory changes. The use of other markers in PET, such as FAMPT for example, may be helpful in differentiating between sarcoid and malignant changes in the future. Ultimately, deciding which diagnostic method is best for each individual patient is the responsibility of the clinician. The decision should be made on the basis of an analysis of possible profits and losses considering the repeatability of the results, availability of the method, its invasiveness, radiation exposure, cost, and possible influence on therapeutic decisions. It is worth emphasizing, that the average radiation dose in the case of X-ray imaging (PA and lateral view) ranged from 0,05–0,25 mSv, in the case of HRCT from 2,1–3,5 mSv, and in the case of PET from 7–11,5 mSv. Bearing in mind that most of the patients with sarcoidosis are between the ages 20 and 40 years old and will never require treatment, the decision about repeated studies involving a high dose of radiation should be made prudently [72].

Conflict of interest

None declared.

References:

1. Statement on sarcoidosis. Joint Statement of the American Thoracic Society (ATS), the European Respiratory Society (ERS) and the World Association of Sarcoidosis and Other Granulomatous Disorders (WASOG) adopted by the ATS Board of Directors and by the ERS Executive Committee, February 1999. *Am J Respir Crit Care Med.* 1999; 160(2): 736–755, doi: [10.1164/ajrccm.160.2.ats4-99](https://doi.org/10.1164/ajrccm.160.2.ats4-99), indexed in Pubmed: [10430755](https://pubmed.ncbi.nlm.nih.gov/10430755/).
2. Bonifazi M, Gasparini S, Alfieri V, et al. Pulmonary sarcoidosis. *Semin Respir Crit Care Med.* 2017; 38(4): 437–449, doi: [10.1055/s-0037-1603766](https://doi.org/10.1055/s-0037-1603766), indexed in Pubmed: [28750459](https://pubmed.ncbi.nlm.nih.gov/28750459/).
3. Kouranos V, Hansell DM, Sharma R, et al. Advances in imaging of cardiopulmonary involvement in sarcoidosis. *Curr Opin Pulm Med.* 2015; 21(5): 538–545, doi: [10.1097/MCP.000000000000195](https://doi.org/10.1097/MCP.000000000000195), indexed in Pubmed: [26176968](https://pubmed.ncbi.nlm.nih.gov/26176968/).
4. Dziedzic DA, Peryt A, Orlowski T. The role of EBUS-TBNA and standard bronchoscopic modalities in the diagnosis of sarcoid-

- osis. *Clin Respir J*. 2017; 11(1): 58–63, doi: [10.1111/crj.12304](#), indexed in Pubmed: [25919969](#).
5. Bugalho A, Szubowski A. Endobronchial ultrasound in sarcoidosis: time to rethink the diagnostic strategy? *Rev Port Pneumol*. 2014; 20(5): 235–236, doi: [10.1016/j.rppneu.2014.05.003](#), indexed in Pubmed: [24997494](#).
6. Pedro C, Melo N, Novais E, Bastos H, et al. Role of bronchoscopic techniques in the diagnosis of thoracic sarcoidosis. *J Clin Med*. 2019; 8(9), doi: [10.3390/jcm8091327](#), indexed in Pubmed: [31466346](#).
7. Culver DA. Diagnosing sarcoidosis. *Curr Opin Pulm Med*. 2015; 21(5): 499–509, doi: [10.1097/MCP.0000000000000201](#), indexed in Pubmed: [26176972](#).
8. Costabel U, Wessendorf TE, Bonella F, et al. Diagnosis of sarcoidosis. *Clin Rev Allergy Immunol*. 2015; 49(1): 54–62, doi: [10.1007/s12016-015-8475-x](#), indexed in Pubmed: [25779004](#).
9. Scadding JG. Prognosis of intrathoracic sarcoidosis in England. *BMJ*. 1961; 2(5261): 1165–1172, doi: [10.1136/bmj.2.5261.1165](#).
10. Muers MF, Middleton WG, Gibson GJ, et al. A simple radiographic scoring method for monitoring pulmonary sarcoidosis: relations between radiographic scores, dyspnoea grade and respiratory function in the British Thoracic Society Study of Long-Term Corticosteroid Treatment. *Sarcoidosis Vasc Diffuse Lung Dis*. 1997; 14(1): 46–56, indexed in Pubmed: [9186989](#).
11. Baughman RP, Shipley R, Desai S, et al. Changes in chest roentgenogram of sarcoidosis patients during a clinical trial of infliximab therapy: comparison of different methods of evaluation. *Chest*. 2009; 136(2): 526–535, doi: [10.1378/chest.08-1876](#), indexed in Pubmed: [19395578](#).
12. Boros PW, Enright PL, Quanjer PH, et al. Impaired lung compliance and DLCO but no restrictive ventilatory defect in sarcoidosis. *Eur Respir J*. 2010; 36(6): 1315–1322, doi: [10.1183/09031936.00166809](#), indexed in Pubmed: [20378598](#).
13. Pietinalho A, Tukiainen P, Haahela T, et al. Early treatment of stage II sarcoidosis improves 5-year pulmonary function. *Chest*. 2002; 121(1): 24–31, doi: [10.1378/chest.121.1.24](#), indexed in Pubmed: [11796428](#).
14. Elicker BM, Kallianos KG, Henry TS. The role of high-resolution computed tomography in the follow-up of diffuse lung disease: Number 2 in the Series “Radiology” Edited by Nicola Sverzellati and Sujal Desai. *Eur Respir Rev*. 2017; 26(144), doi: [10.1183/16000617.0008-2017](#), indexed in Pubmed: [28615307](#).
15. Ley-Zaporozhan J, Ley S. HRCT-Technik mit Low-dose-Protokollen bei interstitiellen Lungenerkrankungen. *Der Radiologe*. 2014; 54(12): 1153–1158, doi: [10.1007/s00117-014-2733-4](#).
16. Hansell DM. High-resolution CT of diffuse lung disease: value and limitations. *Radiol Clin North Am*. 2001; 39(6): 1091–1113, doi: [10.1016/s0033-8389\(05\)70333-x](#), indexed in Pubmed: [11699663](#).
17. Nunes H, Brillet PY, Valeyre D, et al. Imaging in sarcoidosis. *Semin Respir Crit Care Med*. 2007; 28(1): 102–120, doi: [10.1055/s-2007-970336](#), indexed in Pubmed: [17330195](#).
18. Criado E, Sánchez M, Ramírez J, et al. Pulmonary sarcoidosis: typical and atypical manifestations at high-resolution CT with pathologic correlation. *Radiographics*. 2010; 30(6): 1567–1586, doi: [10.1148/rg.306105512](#), indexed in Pubmed: [21071376](#).
19. Lee GM, Pope K, Meek L, et al. Sarcoidosis: a diagnosis of exclusion. *AJR Am J Roentgenol*. 2020; 214(1): 50–58, doi: [10.2214/AJR.19.21436](#), indexed in Pubmed: [31670585](#).
20. Hawtin KE, Roddie ME, Mauri FA, et al. Pulmonary sarcoidosis: the ‘Great Pretender’. *Clin Radiol*. 2010; 65(8): 642–650, doi: [10.1016/j.crad.2010.03.004](#), indexed in Pubmed: [20599067](#).
21. Nakatsu M, Hataba H, Morikawa K, et al. Large coalescent parenchymal nodules in pulmonary sarcoidosis: “sarcoid galaxy” sign. *AJR Am J Roentgenol*. 2002; 178(6): 1389–1393, doi: [10.2214/ajr.178.6.1781389](#), indexed in Pubmed: [12034602](#).
22. Herráez Ortega I, Alonso Orcajo N, López González L. The “sarcoid cluster sign”. A new sign in high resolution chest CT. *Radiologia*. 2009; 51(5): 495–499, doi: [10.1016/j.rx.2009.05.003](#), indexed in Pubmed: [19744682](#).
23. Oda M, Saraya T, Shirai T, et al. Multiple huge “cluster” and “galaxy” signs on chest radiography in a patient with pulmonary tuberculosis. *Respir Case Rep*. 2019; 7(3): e00398, doi: [10.1002/rcr2.398](#), indexed in Pubmed: [30697426](#).
24. Koide T, Saraya T, Tsukahara Y, et al. Clinical significance of the “galaxy sign” in patients with pulmonary sarcoidosis in a Japanese single-center cohort. *Sarcoidosis Vasc Diffuse Lung Dis*. 2016; 33(3): 247–252, indexed in Pubmed: [27758990](#).
25. Heo JN, Choi YoW, Jeon SC, et al. Pulmonary tuberculosis: another disease showing clusters of small nodules. *AJR Am J Roentgenol*. 2005; 184(2): 639–642, doi: [10.2214/ajr.184.2.01840639](#), indexed in Pubmed: [15671390](#).
26. Godoy MCB, Viswanathan C, Marchiori E, et al. The reversed halo sign: update and differential diagnosis. *Br J Radiol*. 2012; 85(1017): 1226–1235, doi: [10.1259/bjr/54532316](#), indexed in Pubmed: [22553298](#).
27. Marchiori E, Zanetti G, Escuissato DL, et al. Reversed halo sign: high-resolution CT scan findings in 79 patients. *Chest*. 2012; 141(5): 1260–1266, doi: [10.1378/chest.11-1050](#), indexed in Pubmed: [22016487](#).
28. Zhan Xi, Zhang L, Wang Z, et al. Reversed halo sign: presents in different pulmonary diseases. *PLoS One*. 2015; 10(6): e0128153, doi: [10.1371/journal.pone.0128153](#), indexed in Pubmed: [26083865](#).
29. Kumazoe H, Matsunaga K, Nagata N, et al. “Reversed halo sign” of high-resolution computed tomography in pulmonary sarcoidosis. *J Thorac Imaging*. 2009; 24(1): 66–68, doi: [10.1097/RTI.0b013e318190476f](#), indexed in Pubmed: [19242310](#).
30. Kouranos V, Wells A, Walsh S. Why do people die from pulmonary sarcoidosis? *Curr Opin Pulm Med*. 2018; 24(5): 527–535, doi: [10.1097/MCP.0000000000000499](#), indexed in Pubmed: [30004991](#).
31. Ziora D, Jastrzębski D, Labus Ł. Advances in diagnosis of pulmonary sarcoidosis. *Pneumonol Alergol Pol*. 2012; 80(4): 355–364, indexed in Pubmed: [22714081](#).
32. Ziora D, Kornelia K, Jastrzębski D, et al. High resolution computed tomography in 2-year follow-up of Stage I sarcoidosis. *Adv Exp Med Biol*. 2013; 788: 369–374, doi: [10.1007/978-94-007-6627-3_50](#), indexed in Pubmed: [23836000](#).
33. Murdoch J, Müller NL. Pulmonary sarcoidosis: changes on follow-up CT examination. *AJR Am J Roentgenol*. 1992; 159(3): 473–477, doi: [10.2214/ajr.159.3.1503008](#), indexed in Pubmed: [1503008](#).
34. Remy-Jardin M, Giraud F, Remy J, et al. Pulmonary sarcoidosis: role of CT in the evaluation of disease activity and functional impairment and in prognosis assessment. *Radiology*. 1994; 191(3): 675–680, doi: [10.1148/radiology.191.3.8184045](#), indexed in Pubmed: [8184045](#).
35. Valeyre D, Nunes H, Bernaudin JF. Advanced pulmonary sarcoidosis. *Curr Opin Pulm Med*. 2014; 20(5): 488–495, doi: [10.1097/MCP.0000000000000075](#), indexed in Pubmed: [25046429](#).
36. Levy A, Hamzeh N, Maier LA. Is it time to scrap Scadding and adopt computed tomography for initial evaluation of sarcoidosis? *F1000Res*. 2018; 7, doi: [10.12688/f1000research.11068.1](#), indexed in Pubmed: [29946423](#).
37. Zappala CJ, Desai SR, Copley SJ, et al. Accuracy of individual variables in the monitoring of long-term change in pulmonary sarcoidosis as judged by serial high-resolution CT scan data. *Chest*. 2014; 145(1): 101–107, doi: [10.1378/chest.12-2479](#), indexed in Pubmed: [24051950](#).
38. Drent M, Vries J, Lelters M, et al. Sarcoidosis: assessment of disease severity using HRCT. *European Radiology*. 2003; 13(11): 2462–2471, doi: [10.1007/s00330-003-1965-x](#).
39. Ors F, Gumus S, Aydogan M, et al. HRCT findings of pulmonary sarcoidosis: relation to pulmonary function tests. *Multidiscip Respir Med*. 2013; 8(1): 8, doi: [10.1186/2049-6958-8-8](#), indexed in Pubmed: [23384173](#).
40. Aleksonienė R, Zeleckienė I, Matačiūnas M, et al. Relationship between radiologic patterns, pulmonary function values and bronchoalveolar lavage fluid cells in newly diagnosed sarcoidosis. *J Thorac Dis*. 2017; 9(1): 88–95, doi: [10.21037/jtd.2017.01.17](#), indexed in Pubmed: [28203410](#).
41. Sulavik SB, Spencer RP, Palestro CJ, et al. Recognition of distinctive patterns of gallium-67 distribution in sarcoidosis. *J Nucl Med*. 1990; 31(12): 1909–1914, indexed in Pubmed: [2266386](#).
42. Leung AN, Brauner MW, Caillat-Vigneron N, et al. Sarcoidosis activity: correlation of HRCT findings with those of 67Ga

- scanning, bronchoalveolar lavage, and serum angiotensin-converting enzyme assay. *J Comput Assist Tomogr.* 1998; 22(2): 229–234, doi: [10.1097/00004728-199803000-00013](https://doi.org/10.1097/00004728-199803000-00013), indexed in Pubmed: [9530385](https://pubmed.ncbi.nlm.nih.gov/9530385/).
43. Malinowska E, Doboszyńska A, Śliwińska A, et al. The use of 67Ga scintigraphy in patients with sarcoidosis. *Nucl Med Rev Cent East Eur.* 2018; 21(1): 59–65, doi: [10.5603/NMR.a2018.0007](https://doi.org/10.5603/NMR.a2018.0007), indexed in Pubmed: [29319141](https://pubmed.ncbi.nlm.nih.gov/29319141/).
44. Tannen BL, Kolomeyer AM, Turbin RE, et al. Lacrimal gland uptake of (67)Ga-gallium citrate correlates with biopsy results in patients with suspected sarcoidosis. *Ocul Immunol Inflamm.* 2014; 22(1): 15–22, doi: [10.3109/09273948.2013.791700](https://doi.org/10.3109/09273948.2013.791700), indexed in Pubmed: [23730797](https://pubmed.ncbi.nlm.nih.gov/23730797/).
45. Piotrowski WJ, Bieńkiewicz M, Frieske I, et al. Somatostatin receptor scintigraphy in sarcoidosis: relation to selected clinical and laboratory markers. *Pol Arch Med Wewn.* 2012; 122(3): 98–106, doi: [10.20452/pamw.1179](https://doi.org/10.20452/pamw.1179), indexed in Pubmed: [22249433](https://pubmed.ncbi.nlm.nih.gov/22249433/).
46. Lebtahi R, Crestani B, Belmatoug N, et al. Somatostatin receptor scintigraphy and gallium scintigraphy in patients with sarcoidosis. *J Nucl Med.* 2001; 42(1): 21–26, indexed in Pubmed: [11197973](https://pubmed.ncbi.nlm.nih.gov/11197973/).
47. Vis R, Malviya G, Signore A, et al. mTc-anti-TNF- α antibody for the imaging of disease activity in pulmonary sarcoidosis. *Eur Respir J.* 2016; 47(4): 1198–1207, doi: [10.1183/13993003.01352-2015](https://doi.org/10.1183/13993003.01352-2015), indexed in Pubmed: [26797030](https://pubmed.ncbi.nlm.nih.gov/26797030/).
48. Galli F, Lanzolla T, Pietrangeli V, et al. In vivo evaluation of TNF-alpha in the lungs of patients affected by sarcoidosis. *Biomol Res Int.* 2015; 2015: 401341, doi: [10.1155/2015/401341](https://doi.org/10.1155/2015/401341), indexed in Pubmed: [25866780](https://pubmed.ncbi.nlm.nih.gov/25866780/).
49. Braun JJ, Kessler R, Constantinesco A, et al. 18F-FDG PET/CT in sarcoidosis management: review and report of 20 cases. *Eur J Nucl Med Mol Imaging.* 2008; 35(8): 1537–1543, doi: [10.1007/s00259-008-0770-9](https://doi.org/10.1007/s00259-008-0770-9), indexed in Pubmed: [18418595](https://pubmed.ncbi.nlm.nih.gov/18418595/).
50. Treglia G, Annunziata S, Sobic-Saranovic D, et al. The role of 18F-FDG-PET and PET/CT in patients with sarcoidosis: an updated evidence-based review. *Acad Radiol.* 2014; 21(5): 675–684, doi: [10.1016/j.acra.2014.01.008](https://doi.org/10.1016/j.acra.2014.01.008), indexed in Pubmed: [24703482](https://pubmed.ncbi.nlm.nih.gov/24703482/).
51. Sobic-Saranovic D, Artiko V, Obradovic V. FDG PET imaging in sarcoidosis. *Semin Nucl Med.* 2013; 43(6): 404–411, doi: [10.1053/j.semnuclmed.2013.06.007](https://doi.org/10.1053/j.semnuclmed.2013.06.007), indexed in Pubmed: [24094707](https://pubmed.ncbi.nlm.nih.gov/24094707/).
52. Mostard RLM, Verschakelen JA, van Kroonenburgh MJ, et al. A predictive tool for an effective use of (18)F-FDG PET in assessing activity of sarcoidosis. *BMC Pulm Med.* 2012; 12(3): 57–447, doi: [10.1186/1471-2466-12-57](https://doi.org/10.1186/1471-2466-12-57), indexed in Pubmed: [22978780](https://pubmed.ncbi.nlm.nih.gov/22978780/).
53. Akaike G, Itani M, Shah H, et al. PET/CT in the diagnosis and workup of sarcoidosis: focus on atypical manifestations. *RadioGraphics.* 2018; 38(5): 1536–1549, doi: [10.1148/rg.2018180053](https://doi.org/10.1148/rg.2018180053), indexed in Pubmed: [30118393](https://pubmed.ncbi.nlm.nih.gov/30118393/).
54. Adams H, Keijsers RG, Korenromp IHE, et al. FDG PET for gauging of sarcoid disease activity. *Semin Respir Crit Care Med.* 2014; 35(3): 352–361, doi: [10.1055/s-0034-1376866](https://doi.org/10.1055/s-0034-1376866), indexed in Pubmed: [25007087](https://pubmed.ncbi.nlm.nih.gov/25007087/).
55. Sobic-Saranovic D, Grozdic I, Videnovic-Ivanov J, et al. The utility of 18F-FDG PET/CT for diagnosis and adjustment of therapy in patients with active chronic sarcoidosis. *J Nucl Med.* 2012; 53(10): 1543–1549, doi: [10.2967/jnumed.112.104380](https://doi.org/10.2967/jnumed.112.104380), indexed in Pubmed: [22879080](https://pubmed.ncbi.nlm.nih.gov/22879080/).
56. Vorselaars ADM, Crommelin HA, Deneer VHM, et al. Effectiveness of infliximab in refractory FDG PET-positive sarcoidosis. *Eur Respir J.* 2015; 46(1): 175–185, doi: [10.1183/09031936.00227014](https://doi.org/10.1183/09031936.00227014), indexed in Pubmed: [25929955](https://pubmed.ncbi.nlm.nih.gov/25929955/).
57. Keijsers RG, Verzijlbergen FJ, Oyen WJ, et al. 18F-FDG PET, genotype-corrected ACE and sIL-2R in newly diagnosed sarcoidosis. *Eur J Nucl Med Mol Imaging.* 2009; 36(7): 1131–1137, doi: [10.1007/s00259-009-1097-x](https://doi.org/10.1007/s00259-009-1097-x), indexed in Pubmed: [19259660](https://pubmed.ncbi.nlm.nih.gov/19259660/).
58. Kaira K, Oriuchi N, Otani Y, et al. Diagnostic usefulness of fluorine-18-alpha-methyltyrosine positron emission tomography in combination with 18F-fluorodeoxyglucose in sarcoidosis patients. *Chest.* 2007; 131(4): 1019–1027, doi: [10.1378/chest.06-2160](https://doi.org/10.1378/chest.06-2160), indexed in Pubmed: [17426205](https://pubmed.ncbi.nlm.nih.gov/17426205/).
59. Dubrey SW, Sharma R, Underwood R, et al. Cardiac sarcoidosis: diagnosis and management. *Postgrad Med J.* 2015; 91(1077): 384–394, doi: [10.1136/postgradmedj-2014-133219](https://doi.org/10.1136/postgradmedj-2014-133219), indexed in Pubmed: [26130811](https://pubmed.ncbi.nlm.nih.gov/26130811/).
60. Moore SL, Teirstein A, Golimbu C. MRI of sarcoidosis patients with musculoskeletal symptoms. *AJR Am J Roentgenol.* 2005; 185(1): 154–159, doi: [10.2214/ajr.185.1.01850154](https://doi.org/10.2214/ajr.185.1.01850154), indexed in Pubmed: [15972416](https://pubmed.ncbi.nlm.nih.gov/15972416/).
61. Sherman JL, Stern BJ, Sherman JL, et al. Sarcoidosis of the CNS: comparison of unenhanced and enhanced MR images. *AJNR Am J Neuroradiol.* 1990; 11(5): 915–923, indexed in Pubmed: [2120996](https://pubmed.ncbi.nlm.nih.gov/2120996/).
62. Brady D, Lavelle LP, McEvoy SH, et al. Assessing fibrosis in pulmonary sarcoidosis: late-enhanced MRI compared to anatomic HRCT imaging. *QJM.* 2016; 109(4): 257–264, doi: [10.1093/qjmed/hcv200](https://doi.org/10.1093/qjmed/hcv200), indexed in Pubmed: [26537956](https://pubmed.ncbi.nlm.nih.gov/26537956/).
63. Chung JH, Little BP, Forssen AV, et al. Proton MRI in the evaluation of pulmonary sarcoidosis: comparison to chest CT. *Eur J Radiol.* 2013; 82(12): 2378–2385, doi: [10.1016/j.ejrad.2013.08.019](https://doi.org/10.1016/j.ejrad.2013.08.019), indexed in Pubmed: [24075784](https://pubmed.ncbi.nlm.nih.gov/24075784/).
64. Craig DA, Colletti PM, Ratto D, et al. MRI findings in pulmonary sarcoidosis. *Magn Reson Imaging.* 1988; 6(5): 567–573, doi: [10.1016/0730-725x\(88\)90131-2](https://doi.org/10.1016/0730-725x(88)90131-2), indexed in Pubmed: [3226240](https://pubmed.ncbi.nlm.nih.gov/3226240/).
65. Chung JH, Cox CW, Forssen AV, et al. The dark lymph node sign on magnetic resonance imaging: a novel finding in patients with sarcoidosis. *J Thorac Imaging.* 2014; 29(2): 125–129, doi: [10.1097/RTI.0b013e3182a4378b](https://doi.org/10.1097/RTI.0b013e3182a4378b), indexed in Pubmed: [24157619](https://pubmed.ncbi.nlm.nih.gov/24157619/).
66. Jenssen C, Annema JT, Clementsen P, et al. Ultrasound techniques in the evaluation of the mediastinum, part 2: mediastinal lymph node anatomy and diagnostic reach of ultrasound techniques, clinical work up of neoplastic and inflammatory mediastinal lymphadenopathy using ultrasound techniques and how to learn mediastinal endosonography. *J Thorac Dis.* 2015; 7(10): E439–E458, doi: [10.3978/j.issn.2072-1439.2015.10.08](https://doi.org/10.3978/j.issn.2072-1439.2015.10.08), indexed in Pubmed: [26623120](https://pubmed.ncbi.nlm.nih.gov/26623120/).
67. Erol S, Anar C, Erer OF, et al. The contribution of ultrasonographic characteristics of mediastinal lymph nodes on differential diagnosis of tuberculous lymphadenitis from sarcoidosis. *Tanaffos.* 2018; 17(4): 250–256, indexed in Pubmed: [31143215](https://pubmed.ncbi.nlm.nih.gov/31143215/).
68. Agrawal SP, Ish P, Goel AD, et al. Diagnostic utility of endobronchial ultrasound features in differentiating malignant and benign lymph nodes. *Monaldi Arch Chest Dis.* 2018; 88(2): 928, doi: [10.4081/monaldi.2018.928](https://doi.org/10.4081/monaldi.2018.928), indexed in Pubmed: [29936788](https://pubmed.ncbi.nlm.nih.gov/29936788/).
69. Cancellieri A, Leslie KO, Tinelli C, et al. Sarcoidal granulomas in cytological specimens from intrathoracic adenopathy: morphologic characteristics and radiographic correlations. *Respiration.* 2013; 85(3): 244–251, doi: [10.1159/000345386](https://doi.org/10.1159/000345386), indexed in Pubmed: [23296305](https://pubmed.ncbi.nlm.nih.gov/23296305/).
70. Hirche TO, Hirche H, Cui XW, et al. Ultrasound evaluation of mediastinal lymphadenopathy in patients with sarcoidosis. *Med Ultrason.* 2014; 16(3): 194–200, doi: [10.11152/nu.2013.2066.163.2hh](https://doi.org/10.11152/nu.2013.2066.163.2hh), indexed in Pubmed: [25110759](https://pubmed.ncbi.nlm.nih.gov/25110759/).
71. Ohana M, Ludes C, Schaal M, et al. What future for chest X-ray against ultra-low-dose computed tomography? *Rev Pneumol Clin.* 2017; 73(1): 3–12, doi: [10.1016/j.pneumo.2016.09.007](https://doi.org/10.1016/j.pneumo.2016.09.007), indexed in Pubmed: [27956084](https://pubmed.ncbi.nlm.nih.gov/27956084/).
72. Martusewicz-Boros MM, Boros PW, Wiatr E, et al. Systemic treatment for sarcoidosis was needed for 16% of 1810 Caucasian patients. *Clin Respir J.* 2018; 12(4): 1367–1371, doi: [10.1111/crj.12664](https://doi.org/10.1111/crj.12664), indexed in Pubmed: [28727253](https://pubmed.ncbi.nlm.nih.gov/28727253/).